Journal of Physics: Conference Series **653** (2015) 012072 doi:10.1088/1742-6596/653/1/012072

Simulation of 3D flows past hypersonic vehicles in FlowVision software

A A Aksenov[1,2], S V Zhluktov[1,2], D V Savitskiy[1], G Y Bartenev[2] and V I Pokhilko[2]

[1] Joint Institute for High Temperatures of the Russian Academy of Sciences, Izhorskaya 13 Bldg 2, Moscow 125412, Russia
[2] TESIS Ltd, Yunnatov 18, Moscow 125256, Russia

E-mail: andrey@tesis.com.ru

Abstract. A new implicit velocity-pressure split method is discussed in the given presentation. The method implies using conservative velocities, obtained at the given time step, for integration of the momentum equation and other convection-diffusion equations. This enables simulation of super- and hypersonic flows with account of motion of solid boundaries. Calculations of known test cases performed in the FlowVision software are demonstrated. It is shown that the method allows one to carry out calculations at high Mach numbers with integration step essentially exceeding the explicit time step.

1. Introduction

The methods developed for numerical integration of the 3D transient Navier–Stokes equations can be broken up into two groups: the methods based on pressure and velocity and the methods based on density and velocity. The methods based on pressure and velocity effectively treat incompressible and weakly compressible flows. Normally, they are not used for simulation of the flows characterized by high Mach numbers. On the contrary, the methods based on density and velocity are used for solving problems of super- and hypersonic aerodynamics. But they cannot treat incompressible and weakly compressible flows. Note that stagnation and recirculation zones occur near a hypersonic vehicle. These zones can be considered as incompressible flows, since the gas velocity here is small. For this reason, development of the methods based on pressure and velocity are of current interest for super- and hypersonic aerodynamics.

Initially, the methods from this group have been designed for simulation of incompressible flows. A pressure correction method has been suggested in [1]. In [2] and [3] it was modified for steady-state problems. An alternative for steady flows is the method of artificial compressibility [4]. It was used in [5–7]. The most popular and actively used methods for integration of "incompressible" Navier–Stokes equations are SIMPLE, SIMPLEC, SIMPLER, PISO. Method SIMPLE (Semi Implicit Method for Pressure Linked Equation) is described in [8]. Explicit split method for solving the Navier–Stokes equations is described in [9,10]. An implicit version of this method is given in [11]. In FlowVision software, the implicit version of the classic split method has been extended to compressible flows [12].

All the aforementioned methods assume solving of the momentum equation with use of the pressure field and conservative velocities (i.e. the velocities satisfying the continuity equation)

at the cell faces obtained at the previous time step. The momentum equation is followed by the Poisson equation for pressure and correction of the velocity field using the pressure field. The drawback of these methods is that the conservative velocities are computed at the end of time step. This is why they cannot be used for solving a problem with boundaries moving with respect to a fixed grid.

The current paper submits a new implicit velocity-pressure split method, which uses conservative velocities obtained at the given time step for solving the Navier–Stokes equations and the other convection-diffusion equations entering the mathematical model. The method is compatible with technologies of moving boundaries. In FlowVision software, moving boundaries occur when a moving body is present in the computational domain, when a conjugate FSI (fluid-structure interaction) problem is solved, when a flow with free or contact surfaces is simulated. The method enables integration of the governing equations at large Mach numbers with time steps essentially exceeding the explicit time step.

2. P-V split approach

Let a computational domain is specified and a finite-volume computational domain is introduced into it. All the sought-for variables (ρ, p, T, $\mathbf{V}$ - density, pressure, temperature and velocity) are stored in the cell centers, i.e. the grid is non-staggered. Besides that specific mass flow rates $\mathbf{W} = \rho\mathbf{V}$ are determined at the cell faces. Let values ρ_c^n, p_c^n, T_c^n, $\mathbf{V}_c^n$ are known at time layer $t = t^n$. Here index c denotes a cell center, index n is the time step number. It is necessary to find values ρ_c^{n+1}, p_c^{n+1}, T_c^{n+1}, $\mathbf{V}_c^{n+1}$ at the next time step. Consider the main equations. The momentum equation reads:

$$\rho_c^{n+1}\mathbf{V}_c^{n+1} - \rho_c^n\mathbf{V}_c^n + \tau\mathbf{CD}\left(\mathbf{W}_f^{n+1}, \mathbf{V}_c^{n+1}\right) = -\tau\nabla p^{n+1}. \tag{1}$$

Here $\mathbf{CD}$ is an operator approximating the convection and diffusion terms in the momentum equation, ∇ is an operator approximating the pressure gradient, $\tau = t^{n+1} - t^n$ is a time step. Subscript f denotes the value of a variable computed at a cell face. The continuity equation:

$$\frac{\rho_c^{n+1} - \rho_c^n}{\tau} + \nabla\mathbf{W}_f^{n+1} = 0. \tag{2}$$

Here ∇ is an operator approximating the divergence of a vector variable. The energy equation:

$$\frac{\rho_c^{n+1}H_c^{n+1} - \rho_c^n H_c^n}{\tau} + CD\left(\mathbf{W}_f^{n+1}, H^{n+1}\right) = \frac{p_c^{n+1} - p_c^n}{\tau}. \tag{3}$$

Here H_c^{n+1} is the total enthalpy at time layer n+1, CD is an operator approximating the convection and diffusion terms in the energy equation. System 1, 2, 3 is completed by the state equations for the considered medium

$$\rho_c^{n+1} = \rho\left(p_c^{n+1}, T_c^{n+1}\right), \tag{4}$$

$$H_c^{n+1} = H\left(p_c^{n+1}, T_c^{n+1}, \mathbf{V}_c^{n+1}\right). \tag{5}$$

Here T_c^{n+1} is the sought-for temperature in a cell center at the given time step.

The methods based on pressure and velocity assume sequential solution of the momentum and pressure equations. The central idea behind this approach consists in introducing an intermediate velocity field, which results from integration of the momentum equation

$$\rho_c^{n+1}\widetilde{\mathbf{V}}_c - \rho_c^n\widetilde{\mathbf{V}}_c + \tau\mathbf{CD}\left(\mathbf{W}_f^n, \widetilde{\mathbf{V}}_c\right) = -\tau\nabla p^n. \tag{6}$$

In general case, the obtained velocity distribution $\widetilde{\mathbf{V}}_c$ does not satisfy the continuity equation. In order to make it conservative, correction must be performed in the cell centers and at the cell faces:

$$\mathbf{W}_c^{n+1} \equiv \rho_c^{n+1}\mathbf{V}_c^{n+1} = \widetilde{\rho}_c\widetilde{\mathbf{V}}_c + \tau\nabla p_c^n - \tau\nabla p_c^{n+1}, \tag{7}$$

$$\mathbf{W}_f^{n+1} \equiv \rho_f^{n+1}\mathbf{V}_f^{n+1} = \widetilde{\rho}_f\widetilde{\mathbf{V}}_f + \tau\nabla p_f^n - \tau\nabla p_f^{n+1}. \tag{8}$$

The pressure at time layer $n+1$ is obtained from the pressure equation. The pressure equation is the result of substituting 7 into the continuity equation:

$$\frac{\rho_c^{n+1}-\rho_c^n}{\tau} + \nabla F\left(\rho_c^{n+1}, \widetilde{\mathbf{V}}_c\right) = \tau\nabla\left(\nabla_f p^{n+1} - \nabla_f p^n\right). \tag{9}$$

Here F is an operator approximating $\mathbf{W}_f$ (the specific mass flow rate through a cell face), ∇_f is the central-symmetric operator approximating the pressure gradient at the cell face using the pressure values in the neighbor cell centers.

The state equation for density provides the following relationship between density and pressure

$$\rho_c^{n+1} = \rho_c^n + \frac{d\rho}{dp}\left(p_c^{n+1} - p_c^n\right). \tag{10}$$

Substitute 10 into 9:

$$\frac{d\rho}{dp}\frac{p_c^{n+1}-p_c^n}{\tau} + \nabla F\left(\rho_c^n + \frac{d\rho}{dp}\left(p_c^{n+1}-p_c^n\right), \widetilde{\mathbf{V}}_c\right) = \tau\nabla\left(\nabla_f p^{n+1} - \nabla_f p^n\right). \tag{11}$$

In the case of incompressible flow ($\partial\rho/\partial p = 0$), 11 becomes an elliptic equation:

$$\tau\nabla\left(\nabla_f p^{n+1} - \nabla_f p^n\right) = \nabla F\left(\rho_c^n, \widetilde{\mathbf{V}}_c\right). \tag{12}$$

In the case of compressible flow, 11 becomes a convection-diffusion equation:

$$\frac{d\rho}{dp}\frac{p_c^{n+1}-p_c^n}{\tau} + \nabla F\left(p_c^{n+1}, \frac{d\rho}{dp}\widetilde{\mathbf{V}}_c\right) - \nabla F\left(p_c^n, \frac{d\rho}{dp}\widetilde{\mathbf{V}}_c\right) = \tau\nabla\left(\nabla_f p^{n+1} - \nabla_f p^n\right) - \nabla F\left(\rho_c^n, \widetilde{\mathbf{V}}_c\right). \tag{13}$$

Hence, pressure propagates over the computational domain with finite velocity $\frac{d\rho}{dp}\widetilde{\mathbf{V}}$. Correct solution of 13 requires the advection operator F to be a high-order monotonous operator. According to the Godunov theorem, it must be non-linear. This makes 13 non-linear with respect to pressure. In FlowVision software, this equation is linearized with use of the deferred-correction method. Explain the method on a simple example. Let we have a high-order linear operator H which is used for integration of the following equation

$$\frac{f^{n+1}-f^n}{\tau} + H(f^{n+1}) = 0. \tag{14}$$

Introduce a linear operator, for instance, the first-order upwind advection operator F_1, and rewrite 14 as follows

$$\frac{f^{n+1}-f^n}{\tau} + F_1(f^{n+1}) = F_1(f^{n+1}) - H(f^{n+1}). \tag{15}$$

Application of the deferred-correction method to 13 yields the following linear equation for pressure

$$\frac{d\rho}{dp}\frac{p_c^{n+1}-p_c^n}{\tau}+\nabla F_1\left(p_c^{n+1},\frac{d\rho}{dp}\widetilde{\mathbf{V}}_c\right)=\tau\nabla\left(\nabla_f p^{n+1}-\nabla_f p^n\right)- \\ -\nabla F\left(\rho_c^n,\widetilde{\mathbf{V}}_c\right)-\nabla F_1\left(p_c^n,\frac{d\rho}{dp}\widetilde{\mathbf{V}}_c\right). \tag{16}$$

It is known that a non-staggered grid produces oscillations in the solution. The effect is explained as follows. The discrete momentum equation includes the approximation of the pressure gradient which does not contain the pressure value in a given cell or contains it with a very small coefficient. On the other hand, the discrete pressure equation includes the approximation of the velocity divergence $\nabla F\left(\rho_c^n,\mathbf{V}_c^n\right)$ in which the coefficient at the velocity in the cell is zero or small. Thus, the discrete equations for velocity and pressure are decoupled in the given cell. This gives birth to so-called checkerboard oscillations. The oscillations are eliminated by means of extending stencil for 16 - see [12–14]. In connection to the scheme discussed, this implies that the pressure gradient at time layer n in 8 is approximated with a higher order of accuracy:

$$\mathbf{W}_f^{n+1}=-F(\rho_c^n,\mathbf{V}_c^n)-F_1\left(p_c^{n+1},\frac{d\rho}{dp}\mathbf{V}_c^n\right)-\tau\nabla\left(\nabla_f p^{n+1}-\nabla_H p^n\right). \tag{17}$$

Here ∇_H is a high-order operator. Correspondingly, the pressure equation changes:

$$\frac{d\rho}{dp}\frac{p_c^{n+1}-p_c^n}{\tau}+\nabla F_1\left(p_c^{n+1},\frac{d\rho}{dp}\mathbf{V}_c^n\right)=\tau\nabla\left(\nabla_f p^{n+1}-\nabla_H p^n\right)- \\ -\nabla F\left(\rho_c^n,\mathbf{V}_c^n\right)-\nabla F_1\left(p_c^n,\frac{d\rho}{dp}\mathbf{V}_c^n\right). \tag{18}$$

Note, that this way of suppressing oscillations makes a steady-state solution dependent on time step. Represent ∇_H as sum $\nabla_H=\nabla_f+\nabla_a$. Here ∇_a is an addition to operator ∇_f having a larger stencil compared to ∇_f. To fix thoughts, consider an incompressible flow. In this case, the steady-state solution of 17 is

$$\mathbf{W}_f^{n+1}=-F(\rho_c^n,\mathbf{V}_c^n)+\tau\nabla_a p^n. \tag{19}$$

We can see that a cell face velocity depends on τ. In order to eliminate the solution dependency on time step, the following expression is used in FlowVision software

$$\mathbf{W}_f^{n+1}=-F(\rho_c^n,\mathbf{V}_c^n)-F_1\left(p_c^{n+1},\frac{d\rho}{dp}\mathbf{V}_c^n\right)-\tau\left(\nabla_f p^{n+1}-\nabla_f p^n-C\nabla_H p^n\right), \tag{20}$$
$$C=\min(1,\tau_{expl}/\tau).$$

Here $\tau_{expl}=\min_i\frac{h_i}{V_i}$ is the explicit time step for the advection equation, h_i is the size of the i-th cell, V_i is the modulus of the velocity in this cell.

3. Final notation of modified split algorithm

Step 1: Solve the convection-diffusion equation for pressure:

$$\frac{d\rho}{dp}\frac{p_c^{n+1}-p_c^n}{\tau}+\nabla F_1\left(p_c^{n+1},\frac{d\rho}{dp}\mathbf{V}_c^n\right)=\tau\nabla\left(\nabla_f p^{n+1}-\nabla_f p^n-C\nabla_H p^n\right)- \\ -\nabla F\left(\rho_c^n,\mathbf{V}_c^n\right)-\nabla F_1\left(p_c^n,\frac{d\rho}{dp}\mathbf{V}_c^n\right),$$

where $\frac{d\rho}{dp}$ is adiabatic compressibility, defined, for instance, like $\frac{d\rho}{dp} = 1/a^2$, where a is speed of sound. *Step 2:* Compute conservative (i.e. satisfying the continuity equation) specific mass flow rates through the cell faces

$$\mathbf{W}_f^{n+1} \equiv \left(\rho^{n+1}V^{n+1}\right)_f = -F(\rho_c^n, \mathbf{V}_c^n) - F_1\left(p_c^{n+1}, \frac{d\rho}{dp}\mathbf{V}_c^n\right) - \tau\left(\nabla_f p^{n+1} - \nabla_f p^n - C\nabla_H p^n\right).$$

Step 3: Compute density

$$\rho_c^{n+1} = \rho_c^n + \frac{d\rho}{dp}\left(p_c^{n+1} - p_c^n\right).$$

This way of computing density provides strict conservation of mass in the computational domain. *Step 4:* Solve the momentum equation

$$\rho_c^{n+1}\mathbf{V}_c^{n+1} - \rho_c^n\mathbf{V}_c^n + \tau\mathbf{CD}\left(\mathbf{W}_f^{n+1}, \mathbf{V}_c^{n+1}\right) = -2\tau\nabla p^{n+1} + \tau\nabla p^n.$$

Step 5: Solve the equations for the turbulent characteristics of the flow (if a turbulent flow is simulated). Solve the convection-diffusion equations for species (if a multi-component flow is simulated). Solve the energy equation

$$\rho_c^{n+1}H_c^{n+1} - \rho_c^n H_c^n + \tau CD\left(\mathbf{W}_f^{n+1}, H^{n+1}\right) = \frac{p_c^{n+1} - p_c^n}{\tau}.$$

Step 6: temperature and corrected density at time layer $n+1$

$$T_c^{n+1} = H^{-1}(p_c^{n+1}, H_c^{n+1})$$
$$\hat{\rho}_c^{n+1} = \rho(p_c^{n+1}, T_c^{n+1}).$$

The accuracy of transient solution at time layer $n+1$ can be improved by computing adiabatic compressibility $d\rho/dp$ through

$$\frac{d\rho}{dp} = \frac{\hat{\rho}_c^{n+1} - \rho_c^n}{p_c^{n+1} - p_c^n}.$$

Then correct density as

$$\rho_c^{n+1} = \hat{\rho}_c^{n+1},$$

and repeating steps 2-6. This option is available in the FlowVision interface.

4. Calculation

4.1. Flow in the Laval nozzle

A 2D (axisymmetric) air flow in the Laval nozzle is considered [15]. The nozzle is a smooth axisymmetric pipe whose radius R depends on the distance along the axis from the inlet as follows:

$$R = \begin{cases} \sqrt{3.6\times10^4 - 1.54\times10^4\cos\left((7.87\times10^4\times x - 1)\times 3.14\right)}, & x < 1.27, \\ \sqrt{2.57\times10^4 - 0.54\times10^4\cos\left((7.87\times10^4\times x - 1)\times 3.14\right)}, & x > 1.27. \end{cases}$$

The nozzle length is 2.4 m. The inlet pressure is 6895 Pa. The inlet temperature is 125 K. The outlet pressure is 5171 Pa. The given pressure drop causes a trans-sonic flow in the nozzle. Calculations in FlowVision software are performed on the grid composed of 5000 cells. The cell size is around 0.1 m. The time step is $\tau = 100\tau_{expl}$, i.e. the CFL number is 100. Though the CFL number is large, the solution development is stable. The calculations are compared against the data from internet-resource [16]. Figure 1 shows the Mach number distribution along the nozzle axis. Figure 2 shows the pressure distribution along the nozzle axis. One can see that the numerical results agree well with the analytical ones.

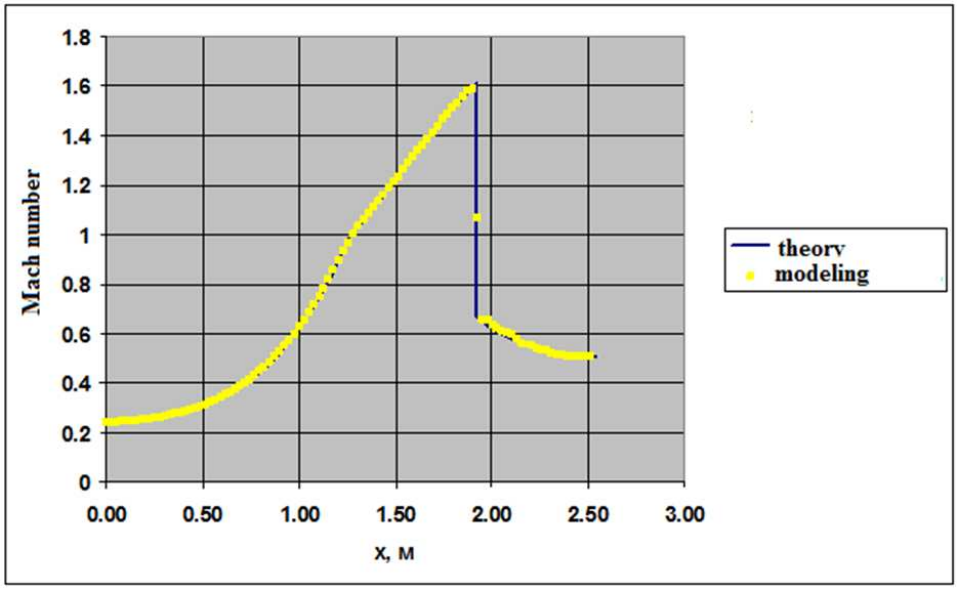

Figure 1. Mach number distribution along the nozzle.

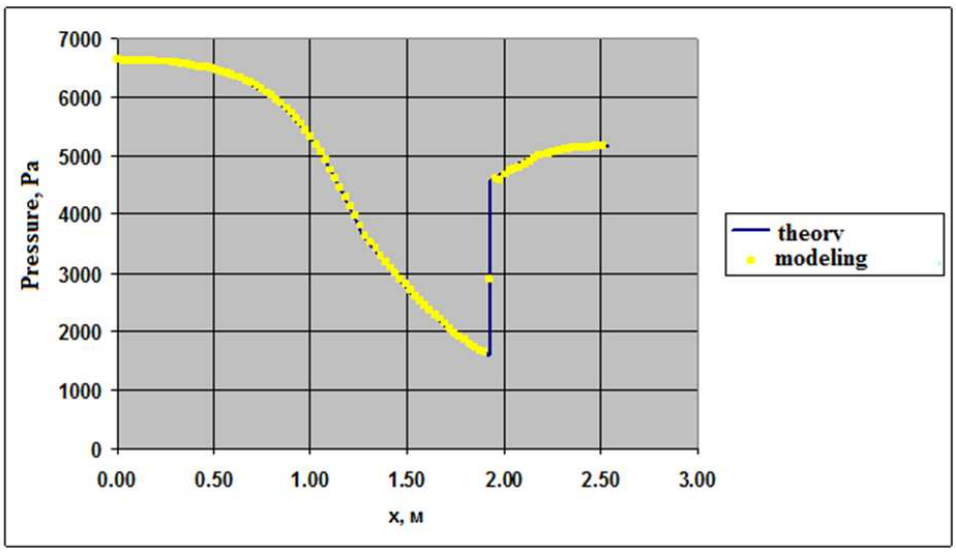

Figure 2. Pressure distribution along the nozzle.

4.2. Hypersonic flow past sphere

Air flow past a sphere is considered. The Mach number is 11.2. The sphere radius is 0.016 m. The investigation is focused on the new method robustness. Therefore chemical reactions are not allowed for. An axisymmetric computational domain is used in this study. The 2D grid consists of 65000 cells. The CFL number equals 10. The corresponding time step provides stable calculations of the given problem. Note that the classic split method allows calculations with time steps characterized by CFL ≤ 1. The Mach number distribution around the sphere is shown in figure 3 In figure 4, the relative pressure distribution over the sphere surface is

compared against the data computed from modified Newton formula [17]

$$p' = \frac{p_b}{p_0} = 1 - \left(1.2 - \frac{1.5}{M_\infty^2}\right)\sin^2\alpha + \left(0.27 - \frac{1.5}{M_\infty^2}\right)\sin^4\alpha. \quad (21)$$

Here p_b is the pressure at the sphere surface, p_0 is the pressure at the stagnation point behind a normal shock wave.

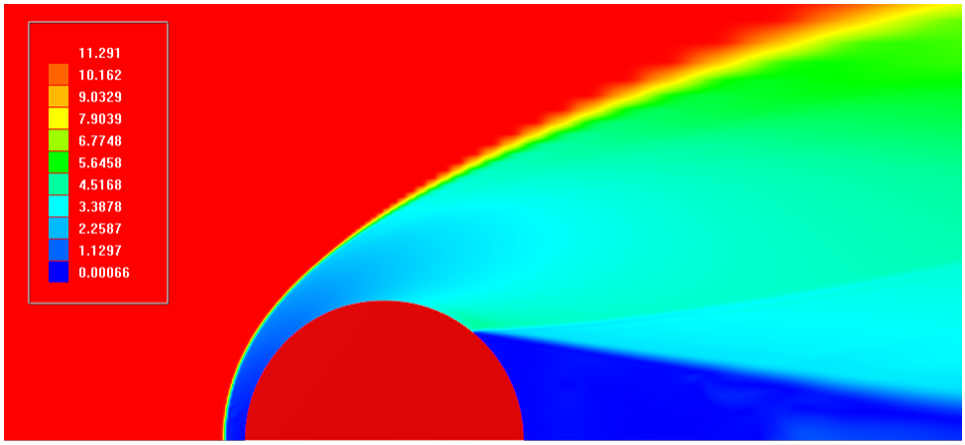

Figure 3. Distribution of the Mach number around sphere.

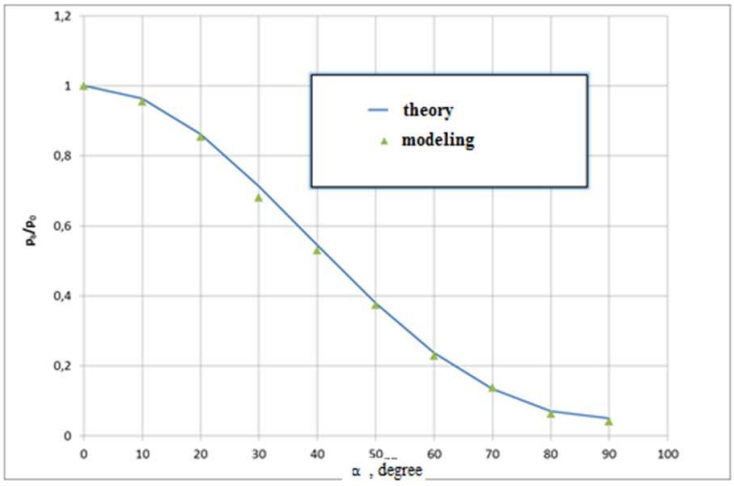

Figure 4. Pressure distribution over the sphere surface.

5. Conclusions

A new method for numerical integration of the Navier–Stokes equations is presented in the given paper. The method allows simulation of fluid and gas flows at arbitrary Mach numbers. The velocity-pressure split approach forms the basis of this method. Compared to the other velocity-pressure split algorithms, the order of solving the momentum and pressure equations is inverted.

In the new method, the pressure equation is solved the first. After that the conservative (i.e. satisfying the continuity equation) mass flow rates through the cell faces are determined. Then this flow rates are used in solving the momentum equation, the energy equation and the other convection-diffusion equations constituting the mathematical model of a given flow. Such an algorithm enables stable calculations with time steps essentially exceeding the explicit time step. The capabilities of the method are demonstrated on two test cases.

Acknowledgments

This work was supported by the Ministry of Education and Science grant No. 14.604.21.0090, 8 July 2014, project ID: RFMEFI60414X0090.

References

[1] Harlow F H and Welch J E 1965 *Phys. Fluids* **8** 2182–2189
[2] Patankar S V and Spalding D B 1972 *Int. J. Heat Mass Transf.* **15** 1787–1806
[3] Patankar S V 1980 *Numerical heat transfer and fluid flow: Computational methods in mechanics and thermal science* (New York: Hemisphere Publishing Corp.)
[4] Chorin A J 1967 *J. Comp. Phys.* **2** 12–26
[5] Peyret R and D T T 1983 *Computational Methods for Fluid Flow* (New York: Springer Verlag)
[6] Chang J L and Kwak D 1984 *AIAA paper* 84–0252
[7] Choi D and Merkle C L 1985 *AIAA J.* **23** 1518–1524
[8] Patankar S V 1981 *Num. Heat Transf.* **4** 409–425
[9] Belotserkovskiy O M, Guschin V A and Schennikov V V 1975 *J. Comp. Math. Math. Phys.* **15** 197–207
[10] Belotserkovskiy O M 1994 *Numerical Simulation in Mechanics of Continuous Media* (Moscow: Nauka)
[11] Aksenov A A, Gudzovskiy A V, Dyadkin A A and Tishin A P 1996 *Izv. Akad. Nauk. Mekh. Zhidk. Gaza* **3** 67–74
[12] Aksenov A, Dyadkin A and Pokhilko V 1998 *ASME-PUBLICATIONS-PVP* **377** 79–83
[13] Armfield S W 1991 *Comp. Fluids* **20** 1–17
[14] Rhie C M and Chow W L 1983 *AIAA J.* **21** 1525–1532
[15] Loytjansky L G 2003 *Mechanics of fluid and gas* (Moscow: Drofa)
[16] http://www.grc.nasa.gov/www/wind/valid/cdv/cdv.html
[17] Lunev B B 2007 *Flow of Real Gases at High Speeds* (Moscow: FIZMATLIT)